Magnetic-based Fano resonance of hybrid silicon-gold nanocavities in the near-infrared region

Xuting Ci,[1] Botao Wu,[1,2] Yan Liu,[1] Gengxu Chen,[1] E Wu,[1] and Heping Zeng[1,*]

[1]*State Key Laboratory of Precision Spectroscopy, East China Normal University, Shanghai, 200062, China*
[2]*btwu@phy.ecnu.edu.cn*
[*]*hpzeng@ phy.ecnu.edu.cn*

Abstract: Direct interference between the orthogonal electric and magnetic modes in a hybrid silicon-gold nanocavity is demonstrated to induce a pronounced asymmetric magnetic-based Fano resonance in the total scattering spectrum at near-infrared frequencies. Differing from the previously reported magnetic-based Fano resonances in metal nanoparticle clusters, the narrow discrete mode provided by the silicon magnetic dipole resonance can be directly excited by external illumination, and greatly enhanced electric and magnetic fields are simultaneously obtained at the Fano dip.

OCIS codes: (160.3918) Metamaterials; (240.6680) Surface plasmons; (290.2200) Extinction.

References and links

1. W. L. Barnes, A. Dereux, and T. W. Ebbesen, "Surface plasmon subwavelength optics," Nature **424**(6950), 824–830 (2003).
2. H. A. Atwater and A. Polman, "Plasmonics for improved photovoltaic devices," Nat. Mater. **9**(3), 205–213 (2010).
3. E. Wu, Y. Chi, B. Wu, K. Xia, Y. Yokota, K. Ueno, H. Misawa, and H. Zeng, "Spatial polarization sensitivity of single Au bowtie nanostructures," J. Lumin. **131**(9), 1971–1974 (2011).
4. M. Song, G. Chen, Y. Liu, E. Wu, B. Wu, and H. Zeng, "Polarization properties of surface plasmon enhanced photoluminescence from a single Ag nanowire," Opt. Express **20**(20), 22290–22297 (2012).
5. K. Ueno, S. Juodkazis, T. Shibuya, Y. Yokota, V. Mizeikis, K. Sasaki, and H. Misawa, "Nanoparticle plasmon-assisted two-photon polymerization induced by incoherent excitation source," J. Am. Chem. Soc. **130**(22), 6928–6929 (2008).
6. B. Wu, K. Ueno, Y. Yokota, K. Sun, H. Zeng, and H. Misawa, "Enhancement of a two-photon-induced reaction in solution using light-harvesting gold nanodimer structures," J. Phys. Chem. Lett. **3**(11), 1443–1447 (2012).
7. F. Hao, Y. Sonnefraud, P. Van Dorpe, S. A. Maier, N. J. Halas, and P. Nordlander, "Symmetry breaking in plasmonic nanocavities: subradiant LSPR sensing and a tunable Fano resonance," Nano Lett. **8**(11), 3983–3988 (2008).
8. J. Ye, F. Wen, H. Sobhani, J. B. Lassiter, P. Van Dorpe, P. Nordlander, and N. J. Halas, "Plasmonic nanoclusters: near field properties of the Fano resonance interrogated with SERS," Nano Lett. **12**(3), 1660–1667 (2012).
9. S. D. Liu, Z. Yang, R. P. Liu, and X. Y. Li, "Multiple Fano resonances in plasmonic heptamer clusters composed of split nanorings," ACS Nano **6**(7), 6260–6271 (2012).
10. S. Liu, M. Zhang, W. Wang, and Y. Wang, "Tuning multiple Fano resonances in plasmonic pentamer clusters," Appl. Phys. Lett. **102**(13), 133105 (2013).
11. Z. Yang, Z. Zhang, Z. Hao, and Q. Wang, "Fano resonances in active plasmonic resonators consisting of a nanorod dimer and a nano-emitter," Appl. Phys. Lett. **99**(8), 081107 (2011).
12. T. Feng, Y. Zhou, D. Liu, and J. Li, "Controlling magnetic dipole transition with magnetic plasmonic structures," Opt. Lett. **36**(12), 2369–2371 (2011).
13. M. Lorente-Crespo, L. Wang, R. Ortuño, C. García-Meca, Y. Ekinci, and A. Martínez, "Magnetic hot spots in closely spaced thick gold nanorings," Nano Lett. **13**(6), 2654–2661 (2013).
14. S. N. Sheikholeslami, A. García-Etxarri, and J. A. Dionne, "Controlling the interplay of electric and magnetic modes via Fano-like plasmon resonances," Nano Lett. **11**(9), 3927–3934 (2011).
15. F. Shafiei, F. Monticone, K. Q. Le, X. X. Liu, T. Hartsfield, A. Alù, and X. Li, "A subwavelength plasmonic metamolecule exhibiting magnetic-based optical Fano resonance," Nat. Nanotechnol. **8**(2), 95–99 (2013).
16. Y. H. Fu, A. I. Kuznetsov, A. E. Miroshnichenko, Y. F. Yu, and B. Luk'yanchuk, "Directional visible light scattering by silicon nanoparticles," Nat. Commun. **4**, 1527 (2013).

#217310 - $15.00 USD Received 18 Jul 2014; revised 11 Sep 2014; accepted 12 Sep 2014; published 22 Sep 2014

17. A. García-Etxarri, R. Gómez-Medina, L. S. Froufe-Pérez, C. López, L. Chantada, F. Scheffold, J. Aizpurua, M. Nieto-Vesperinas, and J. J. Sáenz, "Strong magnetic response of submicron silicon particles in the infrared," Opt. Express **19**(6), 4815–4826 (2011).
18. A. I. Kuznetsov, A. E. Miroshnichenko, Y. H. Fu, J. Zhang, and B. Luk'yanchuk, "Magnetic light," Sci. Rep. **2**, 492 (2012).
19. W. Liu, A. E. Miroshnichenko, R. F. Oulton, D. N. Neshev, O. Hess, and Y. S. Kivshar, "Scattering of core-shell nanowires with the interference of electric and magnetic resonances," Opt. Lett. **38**(14), 2621–2624 (2013).
20. A. E. Miroshnichenko and Y. S. Kivshar, "Fano resonances in all-dielectric oligomers," Nano Lett. **12**(12), 6459–6463 (2012).
21. D. Filonov, A. Slobozhanyuk, A. Krasnok, P. Belov, E. Nenasheva, B. Hopkins, A. Miroshnichenko, and Y. Kivshar, "Near-field mapping of Fano resonances in all-dielectric oligomers," Appl. Phys. Lett. **104**(2), 021104 (2014).
22. K. E. Chong, B. Hopkins, I. Staude, A. E. Miroshnichenko, J. Dominguez, M. Decker, D. N. Neshev, I. Brener, and Y. S. Kivshar, "Observation of Fano resonances in all-dielectric nanoparticle oligomers," Small **10**(10), 1985–1990 (2014).
23. P. Johnson and R. Christy, "Optical constants of the noble metals," Phys. Rev. B **6**(12), 4370–4379 (1972).
24. E. Palik, *Handbook of Optical Constants of Solids* (Academic, 1985).
25. H. van de Hulst, *Light Scattering by Small Particles* (Dover, 1981).
26. F. Hao, E. Larsson, T. Ali, D. Sutherland, and P. Nordlander, "Shedding light on dark plasmons in gold nanorings," Chem. Phys. Lett. **458**(4-6), 262–266 (2008).
27. J. Aizpurua, P. Hanarp, D. S. Sutherland, M. Käll, G. W. Bryant, and F. J. García de Abajo, "Optical properties of gold nanorings," Phys. Rev. Lett. **90**(5), 057401 (2003).
28. H. Wang, F. Tam, N. K. Grady, and N. J. Halas, "Cu nanoshells: effects of interband transitions on the nanoparticle plasmon resonance," J. Phys. Chem. B **109**(39), 18218–18222 (2005).
29. J. Ye, P. Van Dorpe, L. Lagae, G. Maes, and G. Borghs, "Observation of plasmonic dipolar anti-bonding mode in silver nanoring structures," Nanotechnology **20**(46), 465203 (2009).
30. W. Zhang, A. O. Govorov, and G. W. Bryant, "Semiconductor-metal nanoparticle molecules: hybrid excitons and the nonlinear Fano effect," Phys. Rev. Lett. **97**(14), 146804 (2006).
31. P. Fan, Z. Yu, S. Fan, and M. L. Brongersma, "Optical Fano resonance of an individual semiconductor nanostructure," Nat. Mater. **13**(5), 471–475 (2014).
32. B. Luk'yanchuk, A. Miroshnichenko, and Y. Kivshar, "Fano resonances and topological optics: an interplay of far- and near-field interference phenomena," J. Opt. **15**(7), 073001 (2013).
33. E. Prodan, C. Radloff, N. J. Halas, and P. Nordlander, "A hybridization model for the plasmon response of complex nanostructures," Science **302**(5644), 419–422 (2003).
34. V. Giannini, Y. Francescato, H. Amrania, C. C. Phillips, and S. A. Maier, "Fano resonances in nanoscale plasmonic systems: a parameter-free modeling approach," Nano Lett. **11**(7), 2835–2840 (2011).
35. U. Fano, "Effect of configuration interaction on intensities and phase shifts," Phys. Rev. **124**(6), 1866–1878 (1961).

1. Introduction

The light-metal interactions in subwavelength scale can produce localized surface plasmon resonance (LSPR) due to the collective oscillation of free conduction electrons on the metal surface [1]. The resonant excitation of LSPR in metal nanostructures can induce extremely strong localized near field enhancement, and thus has enabled a rich variety of applications in plasmonic photovoltaic cells, surface-plasmon enhanced spectroscopies, photochemistry, photodetectors, and quantum optics [2–6]. Among various novel plasmonic phenomena, Fano resonances in assemblies of strongly-coupled metal nanostructures have attracted considerable interests in recent years, particularly for use in chemical and biological sensing benefiting from sharp spectral features and extreme field localization at nanoscale [7,8]. Owing to the lack of natural magnetism in metal nanomaterials at optical frequencies, magnetic activities are always thought negligible during the light and metal nanomaterials interplay. Therefore Fano resonances have so far mainly focused on purely electric effects in metal nanostructures [7–11].

Very recently there exists a growing interest to explore the artificial magnetic responses of metal nanoparticles when coupled with incident light [12,13]. In fact, it has recently been reported that magnetic-based optical Fano resonances could be observed in closely packed metal nanoparticles arranged in circular loops [14,15]. In planar symmetric nanorings, the *s*-polarized oblique illumination excites both orthogonal electric and magnetic modes, which additively contribute to the total scattering cross section without interference. Symmetry-breaking is utilized as one method to activate the mutual interaction by breaking the orthogonality of the two modes. Such metamaterials with engineered electric and magnetic

#217310 - $15.00 USD Received 18 Jul 2014; revised 11 Sep 2014; accepted 12 Sep 2014; published 22 Sep 2014

resonances may enable many fascinating applications in nanophotonics, but the intrinsic losses and saturation effect strongly affect their overall performance at optical frequencies [16].

Dielectric silicon (Si) nanospheres with high-refractive index have shown outstanding superiority with respect to their metallic analogues that they can support both orthogonal electric and magnetic resonances simultaneously inside the same particle. The optically induced magnetic response in Si nanospheres is due to the circular displacement currents excited by incident light, and the resulted magnetic field oscillating up and down in the middle of the spheres is similar as a "magnetic dipole" [16–18]. However, the dipolar electric and magnetic resonance modes in a single Si nanosphere as well as some other metamaterials like metal-semiconductor core-shell nanowires are noninteracting even though the near fields generated by the two modes can interfere, which can be observed in the forward and backward scattering spectra [16,19]. Recently, magnetic-based Fano resonances in Si nanoparticle heptamers have been demonstrated both experimentally and theoretically, which originated from the interference of the optically-induced magnetic dipole mode of the central Si nanoparticle with the collective mode of the six Si nanoparticles surrounding the central one [20–22].

The coherent interference of electric and magnetic responses is the basis of asymmetric magnetic-based Fano resonances in subwavelength engineered metamaterials. Understanding the underlying physical mechanism of this electromagnetic behavior is of fundamental importance for analysis of the characteristic asymmetric line shape and near-field interactions between the two scattering pathways. In this letter, we theoretically demonstrate a magnetic-based optical Fano resonance in a novel electromagnetically tunable hybrid silicon-gold nanocavity consisting of a Si nanosphere inside the center of an Au nanoring as shown in Fig. 1. Different from the Si heptamers [20–22], the narrow magnetic resonance supported by the central Si nanosphere interferes with the broad electric resonance supported by the Au nanoring, resulting in an apparent magnetic-based Fano dip in the total scattering spectrum in the near-infrared (NIR) region. The spectral shape and position can be tailored by varying the geometrical dimensions and interparticle separation. Also the asymmetric Fano line shape is replicated by calculating the probability to simultaneously excite the dipolar electric and magnetic resonances as well as their coupled state.

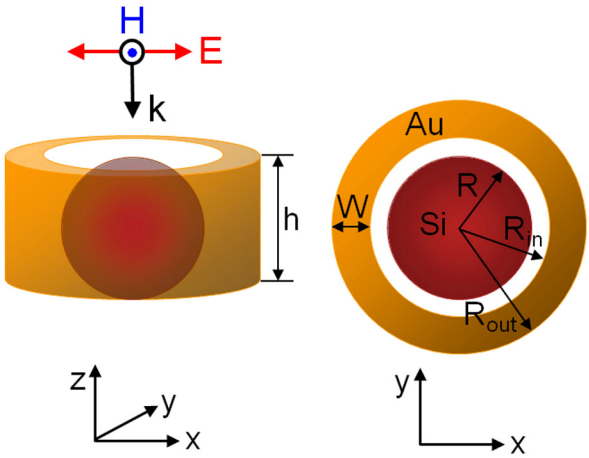

Fig. 1. Schematic geometry of the hybrid silicon-gold nanocavity under normal illumination. The propagation of incident light is along z axis and the polarization of electric field is along x axis. R is the radius of the Si nanosphere, R_{out} and R_{in} are the outer and inner radii of the Au nanoring respectively, $W = R_{out} - R_{in}$ is the width and h is the height of the Au nanoring.

#217310 - $15.00 USD Received 18 Jul 2014; revised 11 Sep 2014; accepted 12 Sep 2014; published 22 Sep 2014

2. Computation details

The numerical simulations are performed by the finite difference time domain (FDTD) Solutions software (Version 8.5, Lumerical Solution, Inc. Canada). The dielectric constants of gold and silicon are taken from Refs [23] and [24], respectively. The schematic geometry of the hybrid silicon-gold nanocavity is illustrated in Fig. 1. The radius of the Si nanosphere is R, located at the center of the Au nanoring with the outer radius R_{out}, inner radius R_{in}, height h, and width $W = R_{out} - R_{in}$. The refractive index of the surrounding matrix is 1. A plane wave total field-scattered field (TFSF) source ranging from 300 to 2000 nm is utilized as the incident light propagating in z direction with electric field polarized in x direction. We use perfectly matched layer (PML) absorption boundary conditions as well as symmetric boundary conditions to reduce the memory requirement and computational time. All the numerical results have been after prior convergence testing.

3. Results and discussion

It has been demonstrated that dielectric Si nanospheres can support strong electric and magnetic dipole responses simultaneously in the visible and NIR regions, where the silicon absorption can be neglected [17]. According to [25], the scattering field of a non-absorbing dielectric sphere illuminated by a plane wave can be decomposed into a multipole series (the so-called Mie expansion) characterized by the electric and magnetic Mie coefficients $\{a_n\}$ and $\{b_n\}$ respectively, defined as

$$a_n = \frac{1}{2}\left(1 - e^{-2i\alpha_n}\right) = i \sin \alpha_n e^{-i\alpha_n}. \quad (1)$$

$$b_n = \frac{1}{2}\left(1 - e^{-2i\beta_n}\right) = i \sin \beta_n e^{-i\beta_n}. \quad (2)$$

where α_n and β_n are the scattering phase-shifts and n is a positive integer, among which a_1 and b_1 are proportional to the electric and magnetic dipoles, a_2 and b_2 to the quadrupoles, and so on. The scattering spectrum of a pure Si nanosphere with the radius R = 150 nm in the NIR region is shown in Fig. 2(a). Two sharp peaks at 1110 and 797 nm are originated from the magnetic dipole (MD) and the magnetic quadrupole (MQ) resonances respectively, while the broad one at 865 nm is ascribed to the electric dipole (ED) resonance [16–18]. To identify the character of a_1 and b_1 coefficients, the near-field distribution profiles in x-z and x-y planes corresponding to the MD and ED resonances are shown in the insets of Fig. 2(a). For the MD resonance, the magnetic field is nearly circularly symmetric inside the nanosphere, while the electric field for the ED resonance is almost linearly polarized along x axis.

Under normal illumination, an isolated Au nanoring only supports dipolar electric resonance modes while higher ordered multipolar ones remain dark [26]. The dipolar plasmon resonances at the inner and outer surfaces of the Au nanoring are coupled strongly giving rise to two plasmon modes: a low-energy symmetric bonding mode and a high-energy asymmetric anti-bonding mode [27]. However, the high-energy anti-bonding mode, typically located near the ultraviolet (UV) region, weakly interacts with incident light due to the weak optical polarizability, and can be further damped by the interband transitions or shadowed by higher ordered multipolar resonance modes [28,29]. Therefore the anti-bonding mode of the Au nanoring is neglected in our simulation. Figure 2(b) displays the scattering spectrum (black curve) of an isolated Au nanoring with R_{out} = 250 nm, R_{in} = 160 nm, and h = 300 nm, which exhibits a very broad electric dipole resonance band at about 1400 nm corresponding to the low-energy symmetric bonding mode as well as an electric quadrupole resonance around 900 nm due to the large Au nanoring dimension.

#217310 - $15.00 USD Received 18 Jul 2014; revised 11 Sep 2014; accepted 12 Sep 2014; published 22 Sep 2014

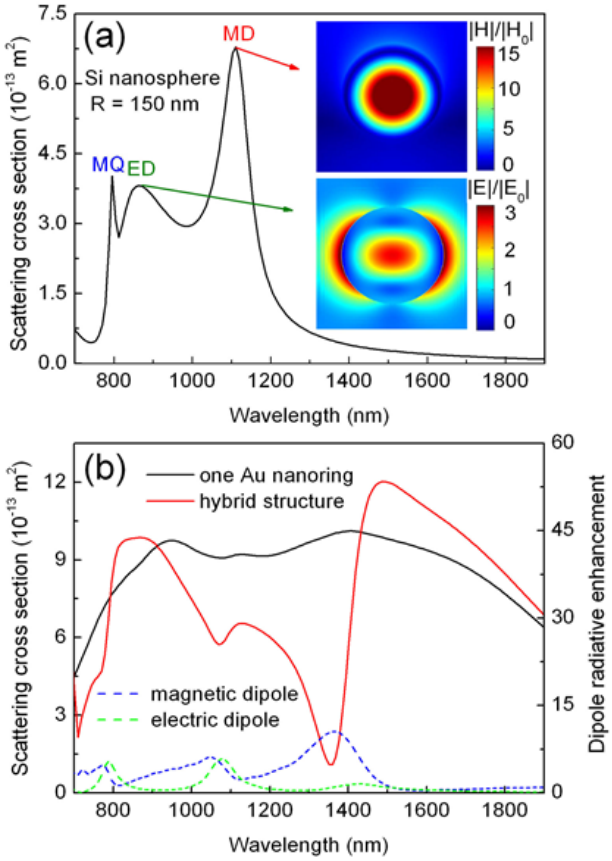

Fig. 2. (a) Scattering spectrum of a pure Si nanosphere with the radius R = 150 nm. The magnetic (in x-z plane) and electric (in x-y plane) near-field distribution profiles corresponding to the MD and ED resonances are shown in the insets. (b) Scattering spectrum (red curve) of the hybrid silicon-gold nanocavity with the outer radius R_{out} = 250 nm, inner radius R_{in} = 160 nm, and height h = 300 nm of the Au nanoring. For comparison, scattering spectrum of the isolated Au nanoring (black curve) is presented. To verify the magnetic essence of Fano dip at 1356 nm, the magnetic (blue dashed curve) and electric (green dashed curve) dipole radiative enhancement spectra when illuminating the hybrid silicon-gold nanocavity using the magnetic and electric dipole light sources respectively are also included.

When the Si nanosphere with the radius R = 150 nm is introduced into the center of the above-mentioned Au nanoring, the magnetic dipole resonance from the Si nanosphere and the electric dipole resonance from the Au nanoring coincide spectrally, resulting in an apparent asymmetric Fano dip at 1356 nm in the total scattering spectrum at NIR frequencies by the coherent interference, as shown by the red curve in Fig. 2(b). Since the Au nanoring exhibits a much broader spectral resonance than the Si nanosphere due to the higher intrinsic losses in Au nanomaterials, the narrow magnetic resonance can be simply tuned to spectrally overlap the broad electric resonance. Meanwhile, the fundamental excitations in the Au nanoring are the surface plasmons with a continuum state, while in Si nanospheres are the discrete interband excitons [30]. The excited resonance modes have different angular momenta, and each angular momentum channel supports a resonant and non-resonant pathway. For subwavelength dielectric Si nanospheres, the resonant pathway dominates the non-resonant one, thus the magnetic dipole mode of the Si nanosphere can be viewed as the discrete resonant pathway, and the electric dipole mode of the Au nanoring plays the role of the continuous non-resonant background. As compared with the non-resonant pathway, the resonant one features an abrupt change of amplitude and phase near the resonance frequency. There is a π phase jump around the magnetic dipole resonance of the Si nanosphere, leading

#217310 - $15.00 USD Received 18 Jul 2014; revised 11 Sep 2014; accepted 12 Sep 2014; published 22 Sep 2014

to the sharp and asymmetric Fano scattering profile originating from the coexistence of both constructive and destructive interferences in the narrow spectral range [31,32]. Clearly an apparent red-shift exists between the MD resonance peak and the induced Fano dip, which can be interpreted in terms of the plasmonic hybridization mechanism [33]. To verify the magnetic essence of the Fano dip at 1356 nm, the hybrid nanocavity is illustrated by a magnetic or electric dipole light source instead of the plane electromagnetic wave, which solely excites the magnetic or electric responses of the hybrid nanocavity. From Fig. 2(b) it is clearly seen that the hybrid nanocavity shows a strong magnetic dipole radiative enhancement around 1356 nm and no electric Fano dip is observed in the electric dipole radiative enhancement spectrum [11], which means that magnetic dipole resonance of the Si nanosphere dominates the contribution to the Fano dip at 1356 nm. Interestingly, the magnetic quadrupole radiative enhancement appears around 1050 nm, corresponding to the shallow Fano dip at 1070 nm in the total scattering spectrum. Unlike the previously reported magnetic-based Fano resonances in properly engineered metal nanoparticle clusters [14,15], the proposed design here does not require any symmetric breaking since the narrow discrete magnetic mode of the Si nanosphere can be directly excited by normal incident light, which makes the Fano resonance generation and tuning more controllable.

We further develop a simple formula based on Fano theory to replicate the simulated Fano line shape for better description of the Fano resonance generation in the hybrid nanocavity [34]. The shape of the resonance caused by the coupling of a discrete state with a continuum has the following form [35]

$$\sigma(\varepsilon) = \frac{(\varepsilon + q)^2}{\varepsilon^2 + 1}. \tag{3}$$

where q is the shape parameter that determines the asymmetry of the profile and is expressed as the excitation probability ratio between the discrete and continuum states. When q is around 1, an asymmetric line-shape is obtained that is typical in many Fano resonance systems. ε is the reduced energy, defined as $2(E - E_d) / \Gamma_d$, which depends on the incident photons energy E, and on the energy of the discrete state E_d, and its width Γ_d. Then, we consider the plasmonic continuum line-shape $\xi(E)$ as a Lorentzian with energy position E_P and width Γ_P given as

$$\xi(E) = \frac{1}{1 + (\frac{E - E_p}{\Gamma_p / 2})^2}. \tag{4}$$

The probabilities that an incident photon excites a discrete state and a continuum are w^2 and $g^2\xi(E)$ respectively, among which the coupling factors are given as $g = (\Gamma_p/2\pi)^{1/2}$ and $w = (\Gamma_d/2\pi)^{1/2}$. Eventually, the probability to directly excite the both noninteracting pathways and their coupled state by external illumination is defined as

$$F(E) = w^2 \times g^2 \xi(E) \times \sigma(\varepsilon). \tag{5}$$

Next, we apply Eq. (5) to replicate the simulated Fano profile of the hybrid nanostructure shown in Fig. 3. For simplicity, we only take the dipolar electric and magnetic resonances into account. The original parameters (λ_p = 1400 nm, Γ_P = 0.74 eV, λ_d = 1110 nm, Γ_d = 0.09 eV, q = 0.25) are obtained from the scattering spectra of the dipolar magnetic and electric resonances from the individual Si nanosphere and Au nanoring respectively, and the calculation result is plotted (red dashed curve). The parameters can be further optimized (λ_p = 1600 nm, Γ_P = 0.74 eV, λ_d = 1325 nm, Γ_d = 0.15 eV, q = 0.25) for better fitting (blue dashed curve). Even though the fitting profile is still rough because the MQ induced Fano resonance and the near-field interaction between the Si nanosphere and Au nanoring when they are brought together are not taken into account and the parameters can't be exactly obtained, it can be seen that the overall shape of the Fano dip is very close to that of the FDTD simulation

#217310 - $15.00 USD Received 18 Jul 2014; revised 11 Sep 2014; accepted 12 Sep 2014; published 22 Sep 2014

(black solid curve). Our theoretical calculation based on Fano theory validates that the magnetic dipole resonance from the Si nanosphere can be directly excited by incident light and serves as the narrow discrete state to interfere with the electric continuum from the Au nanoring, giving rise to the magnetic-based Fano resonance.

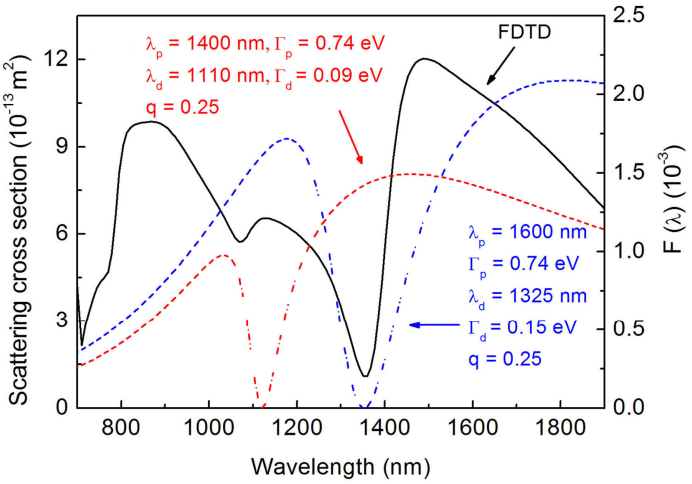

Fig. 3. The FDTD simulation result (black solid curve) and two fitting curves (red and blue dashed curves) calculated by Eq. (5).

The electric and magnetic near-field distribution profiles corresponding to the selected wavelengths of 1120, 1356 and 1478 nm are shown in Fig. 4, which essentially reveal the nature of near-field interactions between the dipolar electric and magnetic modes of the hybrid silicon-gold nanocavity. To facilitate a direct comparison, the fields in Fig. 4 are all plotted in the same scale at the height of $h/2$ in x-y plane. It is interesting to identify that the electric "hottest spots" with highly enhanced localized fields in the gap are obtained at the Fano dip of 1356 nm shown in Fig. 4(a). From the magnetic near-field distributions in Fig. 4(b), it can be seen that the magnetic field of the Si nanosphere at the 1120 nm resonance peak shows a nearly azimuthally symmetric distribution similar to the magnetic field pattern of the isolated Si nanosphere (not shown here), indicating a negligible coupling between the Si nanosphere and the Au nanoring. While at the Fano dip (1356 nm) the magnetic field is enhanced inside the Si nanosphere due to the strong electromagnetic coupling between the Si nanosphere and Au nanoring with a magnetic blank distribution in the vicinity of x axis, which is associated with the magnetic resonant suppression and the destructive interference of the resonant central Si nanosphere and outer Au nanoring [20]. Therefore, it can be concluded that the electromagnetic interference not only influences the scattering spectral line shape, but also modifies the scatterer's original resonance features. And at the 1478 nm resonance peak, the magnetic field distribution is similar to the case at 1356 nm, but its intensity is largely reduced. Obviously the largest magnetic field enhancement also occurs at the Fano dip of 1356 nm. This outstanding character of the hybrid nanostructure that greatly enhanced electric and magnetic near fields can be simultaneously achieved at the Fano dip promises its potential applications in SERS and sensing.

#217310 - $15.00 USD Received 18 Jul 2014; revised 11 Sep 2014; accepted 12 Sep 2014; published 22 Sep 2014

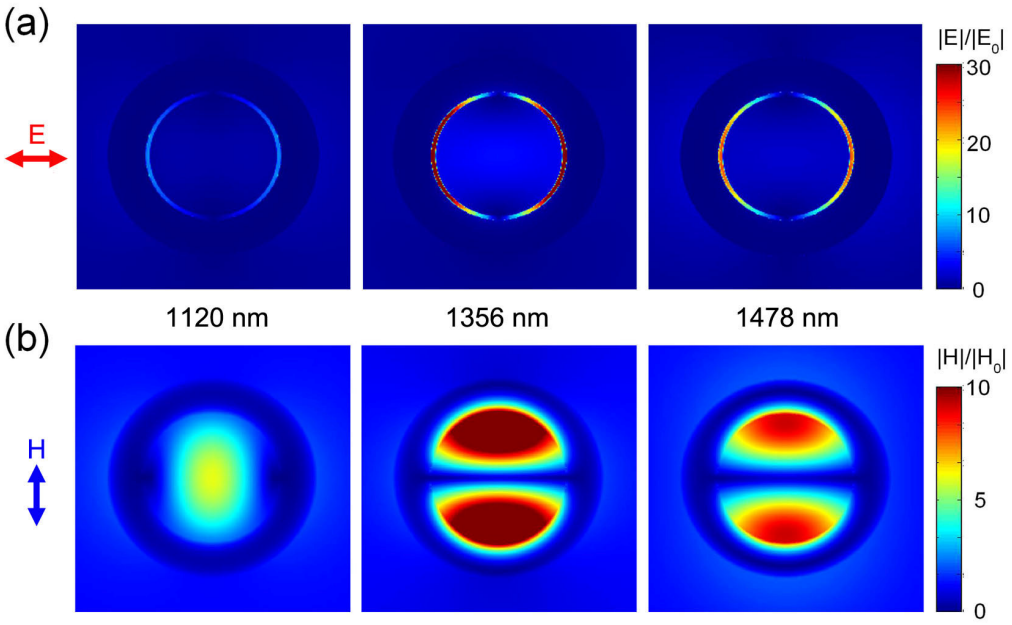

Fig. 4. (a) Electric and (b) magnetic near-field distribution profiles at the height of $h/2$ of the hybrid silicon-gold nanocavity in x-y plane, corresponding to the magnetic-based Fano dip at 1356 nm and the adjacent two resonance peaks at 1120 nm and 1478 nm. The electric and magnetic field polarizations of incident light are indicated at the left sides of (a) and (b) respectively.

Fano line shapes are most pronounced when the two spectrally overlapping scattering modes are of similar magnitudes. The proposed nanocavity in our work allows a convenient tuning of the strengths and positions of the resonance modes. In Fig. 5, we investigate the resonant wavelength and line shape properties of the magnetic-based Fano resonance by varying the structural dimensions and interparticle separation. The scattering spectra dependent on the Si nanosphere radius varying from 125 to 155 nm with the fixed Au nanoring (R_{out} = 250 nm, R_{in} = 160 nm, and h = 300 nm) are shown in Fig. 5(a). With the increase of the Si nanosphere radius the Fano dip exhibits a large red-shift, and becomes deeper and slightly narrower as the resonance frequencies of the Si nanosphere and the Au nanoring move close to each other, concomitantly enhancing the mutual coupling between the broad electric and narrow magnetic resonance modes. When increasing the interparticle distance by simultaneously increasing the outer radius R_{out} and inner radius R_{in} of the Au nanoring from 245 to 275 nm and 155 to 185 nm (maintaining the width W = 90 nm and the Si nanosphere radius R = 150 nm), the Fano dip shows a blue-shift as shown in Fig. 5(b), which can be attributed to the diminishing electromagnetic coupling between the Au nanoring and the Si nanosphere. Compared with the Si nanoparticle heptamers [22], magnetic-based Fano resonance in the hybrid silicon-gold nanocavity is more sensitive to the structural dimensions. These results clearly indicate that the electromagnetic interactions can be efficiently tuned by modifying the geometrical dimensions and interparticle separation of the hybrid nanostructure.

#217310 - $15.00 USD Received 18 Jul 2014; revised 11 Sep 2014; accepted 12 Sep 2014; published 22 Sep 2014

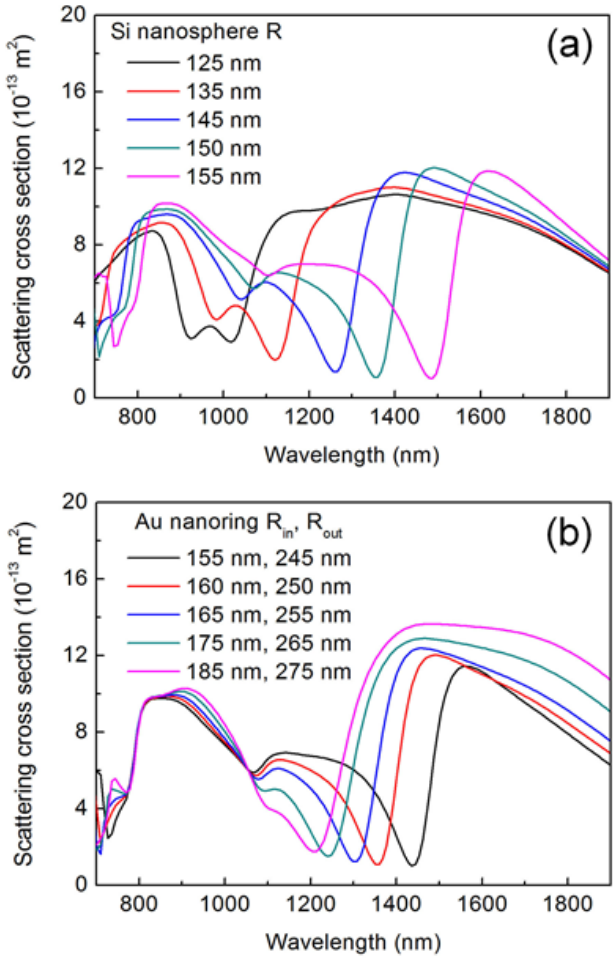

Fig. 5. Scattering spectra of the hybrid silicon-gold nanocavities with (a) different Si nanosphere radii R (125-155 nm) with the fixed Au nanoring (R_{out} = 250 nm, R_{in} = 160 nm, and h = 300 nm) and (b) different Au nanoring outer radii R_{out} (245-275 nm) and inner radii R_{in} (155-185 nm) (maintaining the width W = 90 nm and the Si nanosphere radius R = 150 nm).

4. Conclusion

We have numerically observed magnetic-based Fano resonances arising from the direct interference of electric modes from the Au nanoring and magnetic modes from the Si nanosphere in hybrid silicon-gold nanocavities. The simulated scattering line shape is replicated by calculating the probability to simultaneously excite the both modes and their coupled state in terms of Fano theory. The main advantage of the produced Fano resonance here, compared with the previously reported ones in metal nanoparticle clusters, is that its generation does not need any structure symmetry breaking since the discrete magnetic dipole mode of the Si nanosphere can be directly excited by normal incident light. The Fano dip can be widely tuned by varying the geometrical dimensions and interparticle separation. More especially, greatly enhanced electric and magnetic near-fields are simultaneously obtained at the Fano dip of 1356 nm. The proposed magnetic-based Fano resonance with a high controllability and strong electromagnetic field localization in this letter may enable fascinating applications in surface enhanced spectroscopies, sensing and enhance nonlinear optical response.

#217310 - $15.00 USD Received 18 Jul 2014; revised 11 Sep 2014; accepted 12 Sep 2014; published 22 Sep 2014

Acknowledgments

This work was funded in part by the National Nature Science Fund (11104079 and 61378033), the National Key Scientific Instrument Project (2012YQ150092), the Research Foundation for the Doctoral Program of Higher Education of China (20110076120019), the Program of Introducing Talents of Discipline to Universities (B12024), and the State Key Laboratory of Luminescent Materials and Devices at South China University of Technology.

#217310 - $15.00 USD Received 18 Jul 2014; revised 11 Sep 2014; accepted 12 Sep 2014; published 22 Sep 2014